S. Afr. J. Chem., 2024, 78, 113–121
https://journals.co.za/content/journal/chem/

Enhanced technique for removal of methylene blue dye from water using Luffa microcrystalline cellulose

Vusumuzi Ngwenya, Nqobizitha R. Ndebele, Lindani K. Ncube, Nkosilathi Z. Nkomo, Sithabisiwe Gadlula and Lloyd N Ndlovu*

Department of Fiber and Polymer Materials Engineering, Faculty of Engineering, National University of Science and Technology, Bulawayo, Zimbabwe

ABSTRACT

Methylene blue, a toxic and carcinogenic azo dye, is being discharged as industrial effluent to the environment posing a threat to human health and marine life. Different methods have been developed to alleviate these problems associated with methylene blue. In this work, the adsorption of methylene blue dye was studied using Luffa microcrystalline cellulose (Luffa MCC) under different physicochemical conditions. Luffa MCC was synthesized through a hydrolysis process which entails the extraction of alpha-cellulose from Luffa cylindrica fibers followed by acid treatment for microcrystallisation. The α cellulose extraction was achieved through a pretreatment process of Luffa fibers in NaOH followed by bleaching with H_2O_2 and finally hydrolysis of α-cellulose using HCl. Different methods were used to characterize the properties of Luffa fibers and Luffa MCC. The morphological structure was studied through the use of Fourier Transform Infrared Spectroscopy (FTIR), Scanning Electron Microscope (SEM), Energy Dispersive X-ray spectroscopy (EDS), and Thermogravimetric Analyzer (TGA). Adsorptive removal of methylene blue was studied at different pH, initial dye concentration, adsorbent dosage, temperature and contact time. Maximum adsorption efficiency of 99.69%. of methylene blue was achieved at pH 10 in 180 min. The adsorption kinetics suggests a chemisorption process since it was favoring the pseudo-second-order reaction while the isotherm was best described by Langmuir model which suggests that it was monolayer sorption at a homogenous surface. It can be concluded that adsorption properties were significantly improved after the modification of Luffa fibers.

KEYWORDS

luffa cylindrica fibers; cellulose; adsorption; methylene blue, azo dye, water treatment

Received 6 November 2023, revised 25 January 2024, accepted 11 February 2024

INTRODUCTION

Although industrialization is a necessity for global economic and technological advancement; it does however present problems to the environment through waste disposal. There has been an increase in the usage of azo dyes in the textile industry as well as other sectors such as leather, paper and plastic industries [1,2]. This has resulted in the discharge of large amounts of potentially hazardous effluent into the environment and natural water sources. Environmental agencies globally are becoming more aware and sensitive towards environmental protection. This has given rise to an increase in general awareness about the potential adverse effects of industrial effluents contaminated with various pollutants including azo dye colorants on the environment [3].

Disposal of azo dyes such as methylene blue (MB) is harmful to the environment because they are toxic, that is, they have carcinogenic and mutagenic effects emanating from the azo group [4]. Color is recognized first in wastewater because very small amounts of colorants are highly visible. The effects are on aesthetic merit and transparency of water in addition to gas solubility which is the oxygen transfer mechanism of these water bodies [5,6]. Limited light transmission caused by these colorants affects the photosynthesis process which is essential for the survival of aquatic flora and fauna species [7].

Further, the dye effluent has become a major environmental problem due to the difficulty in elimination of these dyes from wastewater by conventional physicochemical and biological treatment processes [8]. Several effluent treatment methods such as coagulation, filtration, catalysis, electrochemical reduction, and ozonation, have been under study for removal of dyes from water [9,10,11,12]. The major limitations for the application of these methods are capital, availability of resources such as chemicals, space, and technical expertise for carrying out the processes [13]. In comparison the adsorption technique has proven to be an effective method for the removal of dyes from aqueous solutions due to its simplicity, low cost and effectiveness [14,15,16].

Non-conventional natural cellulose based fibers such as Luffa cylindrica are becoming common adsorbents in use due to their environmental friendliness, biodegradability, low cost, and availability[17,18]. Luffa cylindrica is found under the curcubitacea family. It is mainly constituted of cellulose, hemicellulose and lignin, therefore luffa is called as lignocellulosic material. These luffa constituencies variation ratio is dependent on plant origin, weather conditions and soil nature. Basically luffa has a range of cellulose between 55 to 90%, lignin 10 to 23% and hemicellulose 8 to 22% [19,20]. Luffa cylindrica is composed of a fibrous vascular system that allows for usage in removal of water pollutants. From an environmentalist perspective on land management, luffa is biodegradable, renewable and naturally available[17].

Luffa fiber sponge is fast becoming an absolutely necessity because of its potential wide variety industrial applications. Efforts are being made towards the possibility of harnessing, converting and recycling luffa cylindrical fibers into industrial, domestic or technological resources. Luffa sponge is a suitable natural matrix for immobilization of microorganisms and has been successful in the process of bio-sorption of heavy metals from wastewater [21]. This emerging cash crop will improve the economies of many countries in the future because of the potential it possess [22].

Despite being quite cheap, renewable, and biodegradable, with low density and high specific properties, Luffa cylindrica lack applicability due to low adsorption efficiencies caused by hydrophobic impurities such as waxes and pectin [23,24]. However, it can be modified to improve the adsorption properties. Therefore, the overall scope of this study was to modify and quantify the adsorptive properties of Luffa microcrystalline cellulose (Luffa MCC) as a viable option for removal of dyes from wastewater.

*To whom correspondence should be addressed
Email: lloyd.ndlovu@nust.ac.zw

ISSN 1996-840X Online / South African Chemical Institute / https://saci.co.za/journal

https://doi.org/10.17159/0379-4350/2024/v78a16

EXPERIMENTAL

Materials

Luffa cylindrica fibers and distilled (DI) water were sourced locally in Bulawayo, Zimbabwe. Sodium hydroxide (NaOH) ≥ 98%, hydrogen peroxide (H_2O_2) 30%, hydrochloric acid (HCl) 37%, and methylene blue (MB), were all purchased from Sigma Aldrich (Merck), Modderfontein, South Africa and were used as received without further purification.

Preparation of Luffa microcrystalline cellulose

Luffa cylindrica fibers were treated with 4% (w/v) NaOH for 180 min at 80 °C in an oil bath. After which a thorough washing and filtration were performed followed by bleaching with 5.3% (w/v) H_2O_2 for 15 min at 80 °C. The samples were then washed with DI water and treated with 17.5% (w/v) NaOH at 80 °C for 60 min. The extraction process was completed by bleaching it again with H_2O_2 for 15 min. The product was then thoroughly washed and oven-dried for 25 min. Production of Luffa microcrystalline cellulose (Luffa MCC), the obtained α-cellulose was hydrolyzed using 2.5 M HCl at a temperature of 105 °C for 15 min. The Luffa MCC collected was filtered and washed with deionized water to achieve a neutral pH. It was then oven-dried at 60 °C for 60 min and stored in an airtight desiccator.

Equipment and apparatus

Surface morphology was obtained using SEM equipped with EDS, (Model JSM-IT300, JEOL, Akishima, Japan) which was also used for elemental analysis. For SEM analysis, the test was conducted to obtain general microstructure properties on the surface of the test specimen. Before imaging, the samples were gold coated using Cooler Sputter Coater (Model Q300T D, Quorum, Laughton, UK). The gold coating improved the electron conductivity of the samples. FTIR (Model FT-IR100, Perkin Elmer, Shelton, USA) was used for the analysis and detection of functional groups. The samples were tested with an IR spectrum of the sample in the range of 500 – 4000 cm^{-1}. TGA for thermal stability and decomposition was carried out in TA Instrument (Model Universal Analysis 2000, TA Instruments, New Castle, USA). Samples of known mass were subjected to a temperature program at a heating rate of 10 °C/m. A sample was put into the sample pan that is supported by a precision balance in a furnace and was heated and cooled during the experiment. Nitrogen gas was used as a sample purge gas to control the sample environment. The test was carried out from 0-900 °C at a rate of 10 °C/min. The test for water uptake was carried out according to ASTM D570 to determine% weight change on adsorption for Luffa MCC upon exposure to water. Fiber samples were immersed in deionized water for 24 h then filtered through a filter paper then let to sun dry. A comparison was then made using wet weight, Ww and conditioned weight Cw to obtain the% water uptake as shown in Equation 1.

$$\%\ \text{water uptake} = \frac{W_w - C_w}{C_w} \times 100 \quad (1)$$

Adsorption studies

Prior to adsorption studies, stock solutions were prepared by dissolving MB in DI water. Following adsorption, the analysis of the samples was carried out to estimate the MB residual concentration. The samples were collected and then filtered through 11µm pore-sized filter paper. MB concentration was determined using a UV-vis Spectrophotometer (Lambda 650 S, Perkin Elmer, Shelton, USA) at wavelength max (664 nm). All dye solution concentration calculations were done based on the results from the UV-vis comparing them with initial stock concentrations. Physicochemical conditions that affect adsorption were performed in triplicate as (i) effect of pH. (ii) effect of initial dye concentration, (iii) effect of adsorbent dosage, (IV) effect of contact time; and (v) effect of temperature. The pH ranged between 2 and 12, initial dye concentration between 5 and 25 mg/L, adsorbent dosage between 0.1 and 0.30 g, contact time between 30 and 240 min, and temperature between 25 °C and 60 °C. The aforementioned batch experiments were conducted using 50 mL centrifuge tubes which were agitated using a thermostatic shaker model PSI-320 at 150 rpm with one tube filled with 10 mL of dye solution per given time. Solution concentrations were examined using UV-Vis spectrophotometer making use of Equations (2) and (3).

$$\%\text{Ad} = \frac{C_0 - C_e}{C_0} \times 100 \quad (2)$$

$$q_e = \frac{(C_0 - C_e)}{M} \times V \quad (3)$$

Where% Ad is percentage adsorption (dye removal), C_o is initial dye concentration and C_e is the final dye concentration (concentration at equilibrium), and q_e is dye adsorbed (mg/g), V is the volume of the solution used and M is the mass of the Luffa MCC used.

The adsorption kinetics study illustrated the solute uptake rate by Luffa MCC. It was determined using Lagergren pseudo-first and second order model. Lagergren showed that the rate of adsorption of solute on the adsorbent is based on the adsorption capacity. The adsorption kinetics also influence the rate of adsorption. It determines the required time to reach equilibrium for the adsorption process. Kinetic models present information with regards to adsorption pathways and possible involved mechanisms. The pseudo-first-order and pseudo-second-order are expressed in equation (4) and (5) respectively.

$$\log(q_e - q_t) = \log q_e - \frac{k_1}{2.303} t \quad (4)$$

$$\frac{t}{q_t} = \frac{1}{K_2 q_e^2} + \frac{1}{q_e} t \quad (5)$$

Where q_e and q_t are the amounts of adsorbed dye (mg/g), on the adsorbent at equilibrium at time *t*, respectively. K_1 and K_2 are the pseudo first order (min^{-1}) and pseudo second order (mg/g/min) rate constants, respectively.

Adsorption isotherms are also important in explaining how adsorbents interact with adsorbate and suggest the adsorption capacity giving a basic understanding of the mechanism involved. Langmuir and Freundlich's models are most commonly used to describe the adsorption isotherm. Freundlich's adsorption isotherm model considers a heterogeneous adsorption surface with unequal available sites with different energies of adsorption. Freundlich adsorption isotherm is represented in Equation 6.

$$\log q_e = \log K_f + \frac{1}{n}(\log C_e) \quad (6)$$

Where q_e represents the adsorbed amount of dye molecules at equilibrium time (mg/g), C_e represents the equilibrium concentration of the dye in solution (mg/L), K_f represents the capacity of the adsorbent and *n* represents the intensity of adsorption constant for Freundlich. The plot of log q_e against log C_e is used to determine the K_f and *n* from intercept and slope respectively. Langmuir adsorption isotherm assumes that adsorption happens at specific homogeneous sites within the adsorbent, and it has been used successfully for many adsorption processes of monolayer adsorption. Langmuir equation is expressed by equation 7.

$$\frac{C_e}{q_e} = \frac{C_e}{q_m} + \frac{1}{K_a C_e} \quad (7)$$

Where q_e represents the amount of dye adsorbed at equilibrium time (mg/g), C_e represents the equilibrium concentration of dye in solution (mg/L), q_e represents the maximum adsorption capacity (mg/g) and K_a represents the isotherm constants for Langmuir.

RESULTS AND DISCUSSION

Yield of microcrystalline cellulose

The percentage yield of microcrystalline cellulose obtained from the Luffa cylindrical fibers was approximately 58.31%. This percentage yield is comparable to that reported by other researchers who obtained a 61% yield of MCC from Luffa [25]. Furthermore, the 58.31% yield obtained in this study is higher than what was reported by Ejikeme [26] who obtained a 21% extraction yield of MCC from raw cotton of Cochlospermum planchonii and 25.3% from orange mesocarp. Therefore, the MCC yield obtained in this study is relatively high enough to motivate the commercialization of the farming and extraction of Luffa MCC for effluent treatment and other possible applications.

Water uptake

The test for water uptake was carried out according to the standard ASTM D570. A water absorption test was used to determine the amount of water absorbed under the specified conditions. Water uptake was done to investigate the performance of Luffa fibers and Luffa MCC in water and humid environments. The Luffa fibers and Luffa MCC both had a dry weight of 0.15 g. After 24 hours of being immersed in DI water, Luffa fibers recorded a weight of 1.38 g while Luffa MCC recorded a weight of 1.43 g. Using Equation 1, the calculated results showed a percentage water uptake of 82% and 85.33% for Luffa fibers and Luffa MCC respectively. Cellulose based materials contain hydroxyl groups which are responsible for water absorption and hydrophilicity. Saikia [27] investigated cellulosic fibers for water absorption and noted that bowstring hemp had 62%, okra had 64% and betel nut had 38%. They further affirmed the relationship of water uptake to the cellulosic content and hydrophilic functional groups present. In this study, both Luffa fibers and Luffa MCC had relatively high water uptake. However, Luffa fibers had lower water uptake due to waxes and hydrophobic impurities contained in the fiber structure. The treatment process on Luffa fibers removed waxes and other hydrophobic impurities to produce Luffa MCC which are highly polar and hydrophilic. As such, Luffa MCC had the highest water uptake compared to Luffa fibers.

FTIR analysis

The FTIR spectra for Luffa fibers and Luffa MCC is displayed in Figure 1. It can be noted that the spectra are exhibited OH stretching absorption at approximately 3400 cm^{-1}, CH stretching absorption 2900 cm^{-1}, C=O stretching absorption at 1650 cm^{-1}, and C-O stretching absorption at approximately 1100 cm^{-1}.[28] Luffa fibers and Luffa MCC are characterized by the same functional groups as cellulose which proves the presence of cellulose in both materials. Moreover, this indicates that chemical treatment of Luffa fibers did not alter the chemical structure of the cellulosic fiber.

SEM and EDS

Figure 2 displays the morphology of Luffa fibers and Luffa MCC obtained using SEM analysis. Figure 2a shows a regular structure having discreet net fibrils, where the presence of lignin, hemicelluloses, and wax contributes toward the homogeneous morphology of the natural composite structure of Luffa fiber.

On the other hand, Figure 2b shows the micrograph of Luffa MCC which have visible surface roughness caused by chemical treatment done to remove hemicellulose and waxes. The surface roughness increases the surface area of the Luffa MCC and contributes towards improved dye adsorption capacity. The increased surface area is proportional to the increase in the number of active sites that consist of OH functional groups on which the dye molecule can be attracted. This is confirmed in the FTIR and EDS results in Figure 1 and Figure 3, respectively. It can be noticed in Figure 3 that Au was detected in the Luffa samples. This is due to Au coating which was done during the sample preparation.

Figure 4 shows carbon and oxygen distribution on Luffa MCC. Fig 4b shows carbon and oxygen elemental distribution in the Luffa MCC chemical chain. While Fig 4c and 4d are separate carbon and oxygen distribution respectively. These results reveal a uniform distribution of the carbon and oxygen elements in the cellulose structure. The uniform distribution favors an even distribution of OH groups that

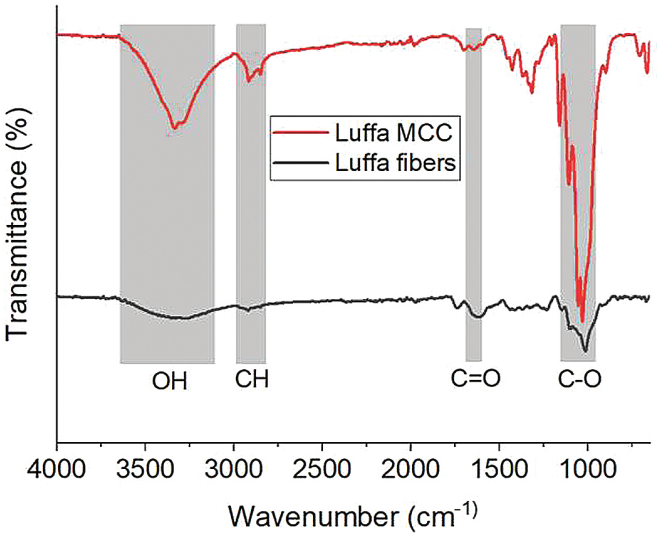

Figure 1. FTIR spectra for Luffa fibers and Luffa MCC

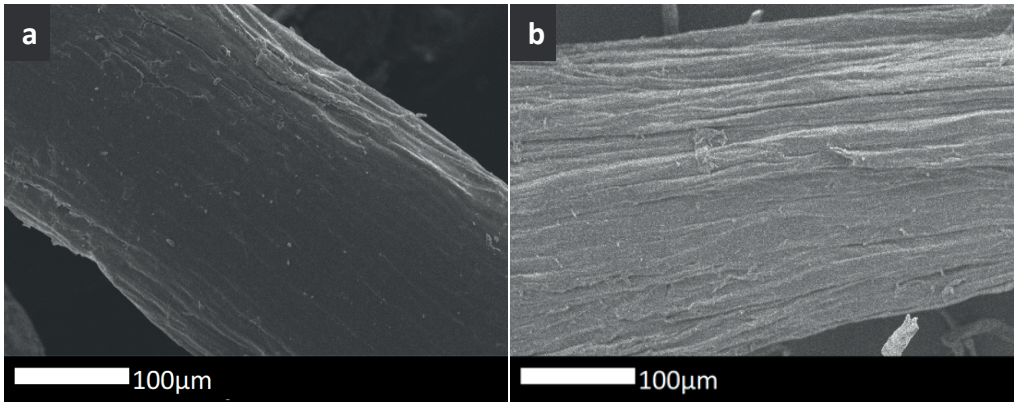

Figure 2. SEM micrographs for Luffa fiber (a) and Luffa MCC (b)

S. Afr. J. Chem., 2024, 78, 113–121
https://journals.co.za/content/journal/chem/

facilitate MB dye adsorption.

Thermogravimetric analysis

The TGA curves for Luffa fibers and Luffa MCC are shown in Figure 5. The obtained thermograms are similar to those reported by other researchers.[29,30,31] The initial weight loss of approximately 5% can be attributed to the evaporation of water and loosely bound volatile matter on the surface of the materials. Luffa fibers start degrading at 200 °C with about 60 °C temperature increase to approximately 260 °C and loses about 5% of its weight. The fibers start the major decomposition at approximately 250 °C with an exponential weight loss. The decomposition process for the Luffa fibers is slowed down for the 40% weight at 350 °C. This process may be attributed to the carbonization of the Luffa fibers.

Luffa MCCs lose 5% of its weight from the start to approximately 330 °C. Further loss in weight may be attributed to pyrolysis, that is, Luffa MCCs were observed to decompose in the 310 °C to 340 °C region. The loss is approximately 70% with a sharp weight decrease which is the main thermal decomposition Luffa MCC. This is attributed to main chain degradation due to the breakdown of glycosidic bonds followed by the decomposition of volatile dehydrated compounds in Luffa MCC. The final stage of mass loss ranges from the 350 °C to 520 °C region and is ascribed to sample carbonization as a result of the complete degradation and decomposition of the Luffa MCC sample. The chemical treatment process increased the main chain decomposition temperature from 250 °C to 350 °C while it also allows holding of volatile matter as seen through the stability of Luffa fibers

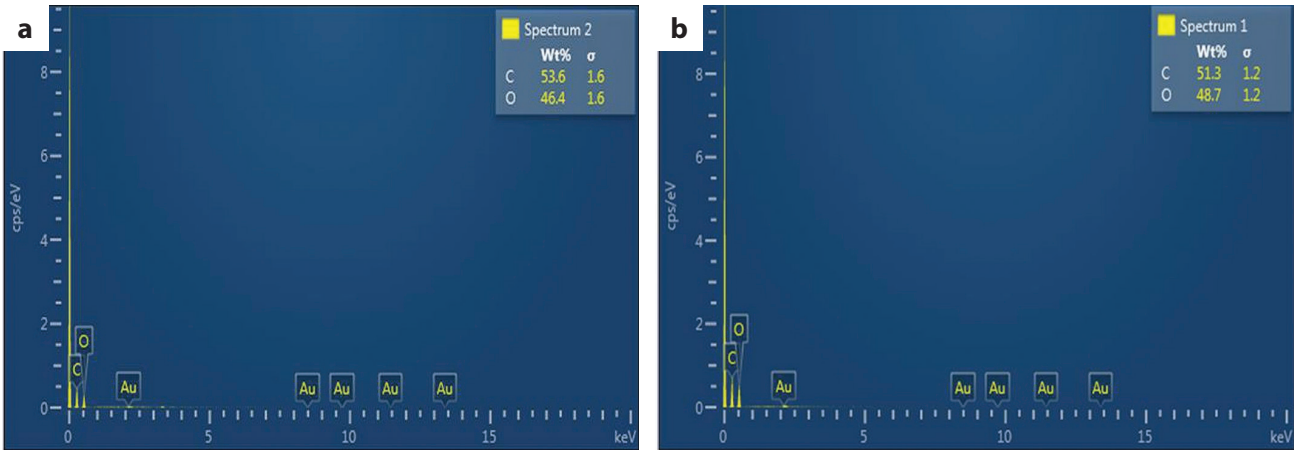

Figure 3. EDS for Luffa fiber (a) and Luffa MCC (b)

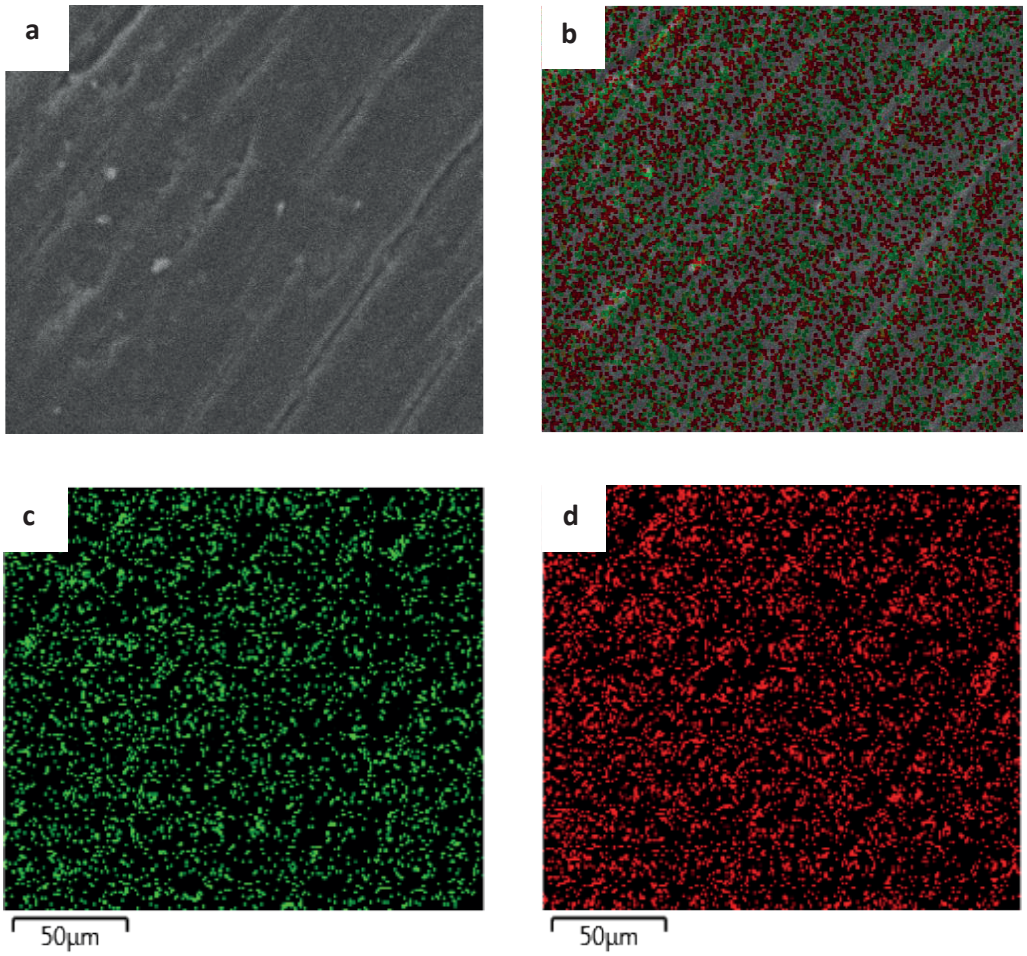

Figure 4. EDS mapping for Luffa MCC showing electron image (a), layered image (b), and elemental distribution of carbon (c) and oxygen (d)

performing better at the beginning than Luffa MCC.

Adsorption data

Effect of pH and concentration

The results on effect of pH on the adsorption of MB using Luffa fibers and Luffa MCC are shown in Figure 6. It can be noticed that adsorption efficiency increased with the increase in pH which showed a significant influence of pH on the adsorption efficiency of the sorbent [32]. Higher adsorption efficiency was observed at alkaline pH, having pH 10 being the highest having an adsorption efficiency of 98.5%. At acidic pH the hydroxyl groups of the cellulose structure of Luffa MCC are protonated and repel the positively charged MB dye ions leading to low adsorption efficiency. However, at alkaline pH the Luffa MCC are deprotonated increasing affinity with the MB dye molecules. Mostly the dye molecules are adsorbed through hydrogen bonding between hydroxyl groups of Luffa MCC and nitrogen in MB dye molecules.

The effect of the initial dye concentration of MB was studied as presented in Figure 6. Adsorption efficiency for Luffa MCC based on all dye concentrations remained significantly high as it stayed above 90%. The concentration with the highest efficiency was 10 mg/L having 99.18% and the lowest was 25 mg/L having 90.70%. Concentrations of 5ppm to 20ppm appear to reveal that the adsorption sites are in abundance while at 25 mg/L the fibers appear to have suffered saturation and thus a slight decrease in adsorption efficiency. Luffa MCC had a large surface area which provided an adequate surface for interaction with the dye molecules promoting adsorption efficiency of above 90%. A similar trend is seen in adsorption using Luffa fibers. However, Luffa fibers recorded lower adsorption efficiency of between 38.9% and 55% across dye concentrations. This could be due to presence of hydrophobic impurities in Luffa fibers which prevent access to most of the adsorption sites. It can therefore be concluded that dye concentration has little effect on the dye adsorption efficiency of the adsorbents.

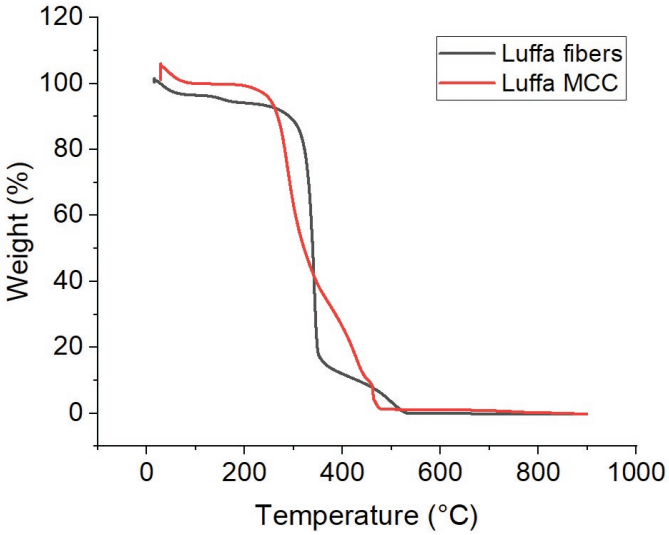

Figure 5. TGA thermograms for Luffa fibers and Luffa MCC

Effect of dosage and contact time

On the effect of adsorbent dosage, the study was carried out using dosage weights 0.10, 0.15, 0.20, 0.25 and 0.30 g having 0.30 g showing the highest adsorption efficiency. Generally, as seen in Figure 7, dosage had an effect on the adsorption efficiency as 0.1 g and 0.30 g recorded 90.90% and 98.97% respectively for Luffa MCC. Similarly, Luffa fibers showed lowest adsorption capacity of 49.38% for 0.10 g and highest adsorption efficiency of 68.71% for 0.30 g. An increase in adsorption capacity with an increase in dosage was expected since the number of adsorption sites (hydroxyl groups) increased with dosage [33].

Contact time has a significant effect on the adsorption efficiency of the sorbent. As displayed in Figure 7, the experiment was run for a total of 240 min and showed an increase in adsorption efficiency as the time increased from 30 minutes to 240 min. Thus, Luffa fibers adsorption efficiency increased from 14.11% to 74.74% while for Luffa MCC the efficiency increased from 64.62% to 99.64%. The increase in adsorption efficiency may be attributed to the increased contact time which allows the diffusion and adhesion of dye molecules into Luffa fibers and Luffa MCCs.

Effect of temperature

Temperature is a significant Physico-chemical process parameter because it shows the nature of the reaction taking place that is either an exothermic or endothermic process. In Figure 8 temperature change had a significant effect on the adsorption efficiency of Luffa fibers and Luffa MCC, that is, increasing temperature decreased the adsorption efficiency.

Luffa fibers adsorption efficiency was 50.72% at 25 °C and it decreased to 44.99% at 60 °C. on the other hand Luffa MCC decreased from 94.89% to 72.80% when the temperature was increased from 25 °C to 60 °C. Increasing temperature reduced affinity between Luffa and MB dye molecules which led to reduction in adsorption capacity. Thus, an increase in temperature weakened the adsorptive forces between the active sites of the dye molecules and the adsorbent

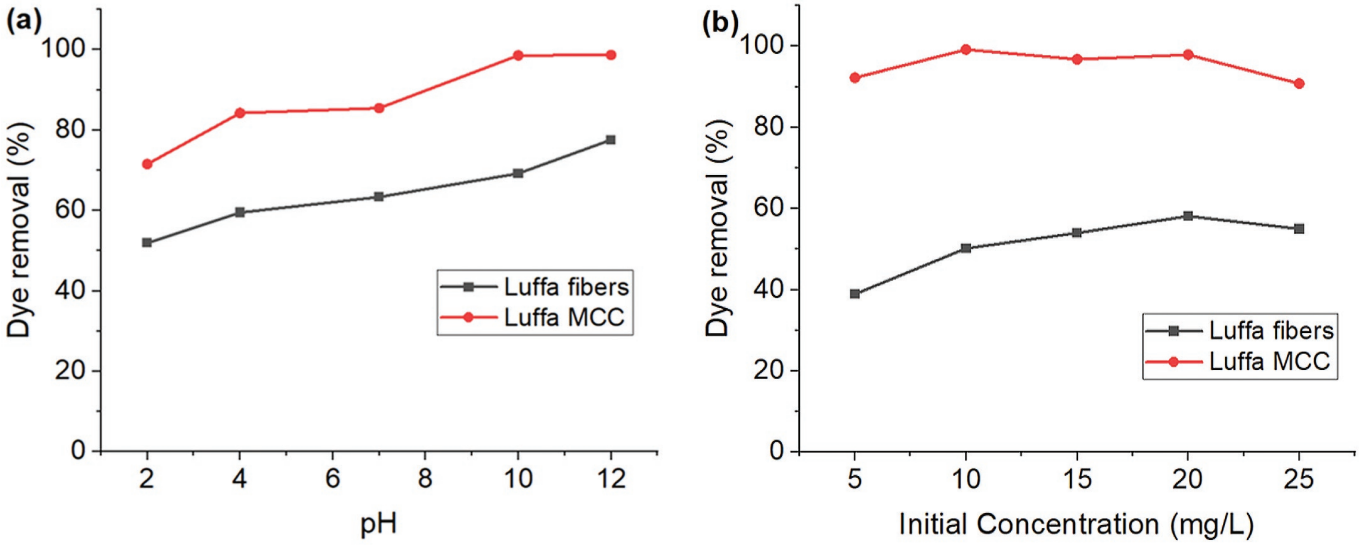

Figure 6. Effect of pH (a) and initial concentration (b) on adsorption of methylene blue

resulting in reduction in adsorption efficiency.[34] Therefore, the decrease in adsorption efficiency is attributed to adsorption being an exothermic process.

Adsorption kinetics and isotherms

Figure 9 represent the pseudo-first and second-order kinetic models and also Langmuir and Freundlich isotherm models for the dye removal of MB while Table 1 summarizes their parameters.

It is noted that the pseudo-second-order model has the highest correlation R^2 of 0.99 compared to 0.88 of the pseudo-first-order model. This means that the reaction favors the pseudo-second-and hence it implies that the reaction involved is a chemisorption reaction. The pseudo-second-order reaction is greatly influenced by the amount of dye on the adsorbent's surface and the amount of dye adsorbed at equilibrium. The adsorption rate is directly proportional to the number of active surface sites. For the isotherm data, it is noted that the removal of MB dye is best suited in the Langmuir isotherm model as R^2 is highest (0.93) compared to 0.88 of Freundlich model. This means that the reaction relatively occurs by monolayer adsorption at a homogeneous surface.

Proposed adsorption mechanism

Figure 10 shows the proposed mechanism for the adsorption of MB on Luffa MCC adsorbents. The adsorption capacity and efficiency of Luffa MCC is highly dependent on the number of adsorption sites and functional groups of both Luffa MCC and MB dye molecules.

Luffa MCC is rich with OH groups while MB dye molecules have abundant nitrogen and sulfur containing functional groups. The adsorption of MB by Luffa MCC is due to hydrogen bonding. The Luffa MCC structure is rich with OH groups which form hydrogen bonds with the nitrogen and sulfur in the MB dye molecules.

The FTIR spectra for Luffa MCC and Luffa MCC/MB are displayed in Figure 11. It can be noted that the spectra are exhibited by C-O stretching absorption at approximately 1100 cm^{-1}, C=O stretching absorption at approximately 1650 cm^{-1}, CH stretching absorption at approximately 2900 cm^{-1} and OH stretching absorption at approximately 3400 cm^{-1}. The Luffa MCC/MB spectrum is showing a drastic change on the main band ascribed to OH functional groups. Tan and colleagues stated that the presence of the OH main band after adsorption may be related to the interaction between cellulose and water in MB dye solution. The presence of MB dye is proven by a band at 1626 cm^{-1} belonging to C=N bond. This proved that the MB dye molecules were attached to the active site of Luffa MCCs.

Regeneration studies

This process allows the usage of the adsorbents several times before there is a significant change in the adsorption efficiency. In this experiment, desorption of MB from Luffa MCC was done using methanol. Moreover, other solvents such as acetonitrile, ethanol and HCl can be investigated for the desorption of MB from Luffa MCC.

After each adsorption cycle Luffa MCC were placed in a beaker of methanol for 3 h followed by washing with DI water. After washing the Luffa MCC were reused for adsorption of MB. The results in Figure 12 show that the adsorption efficiency decreased per cycle carried with first cycle recording 99.69% and fifth cycle recording 91.52%. Therefore, these results support the reusability of Luffa MCC on removal of MB from water.

CONCLUSION

The present study shows that Luffa MCC were successfully extracted from Luffa cylindrical fibers and the obtained yield of 58.31% is high enough to promote the commercialization of the method. The study further shows that Luffa MCC can be efficiently used as an adsorbent for the removal of MB from aqueous solutions. The obtained maximum adsorption efficiency was 99.69% and was mostly due to hydrogen bonding. MB adsorption was found to be influenced by pH, concentration, dosage, exposure time and temperature Luffa MCC

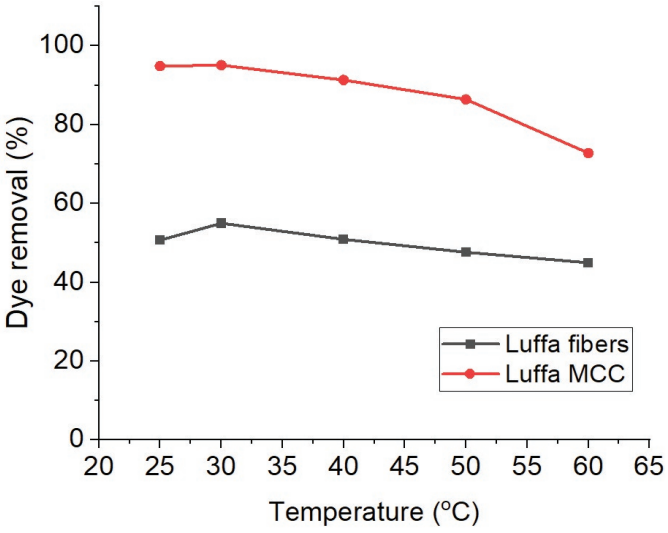

Figure 8. Effect of temperature on adsorption of methylene blue

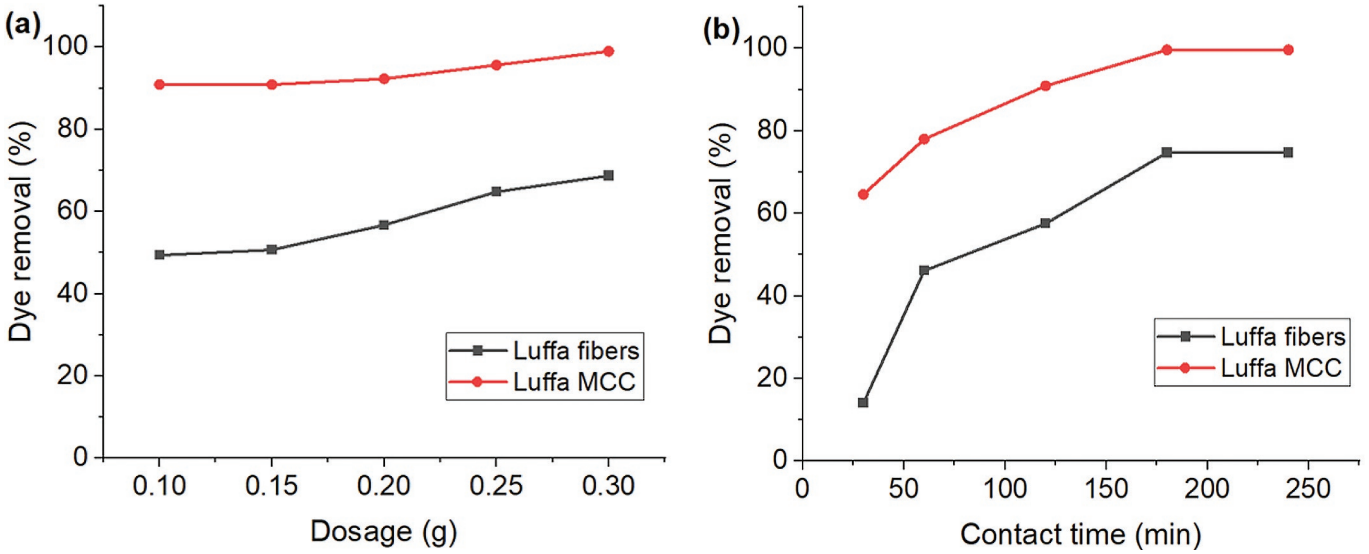

Figure 7. Effect of adsorbent dosage (a) and contact time (b) on methylene blue adsorption

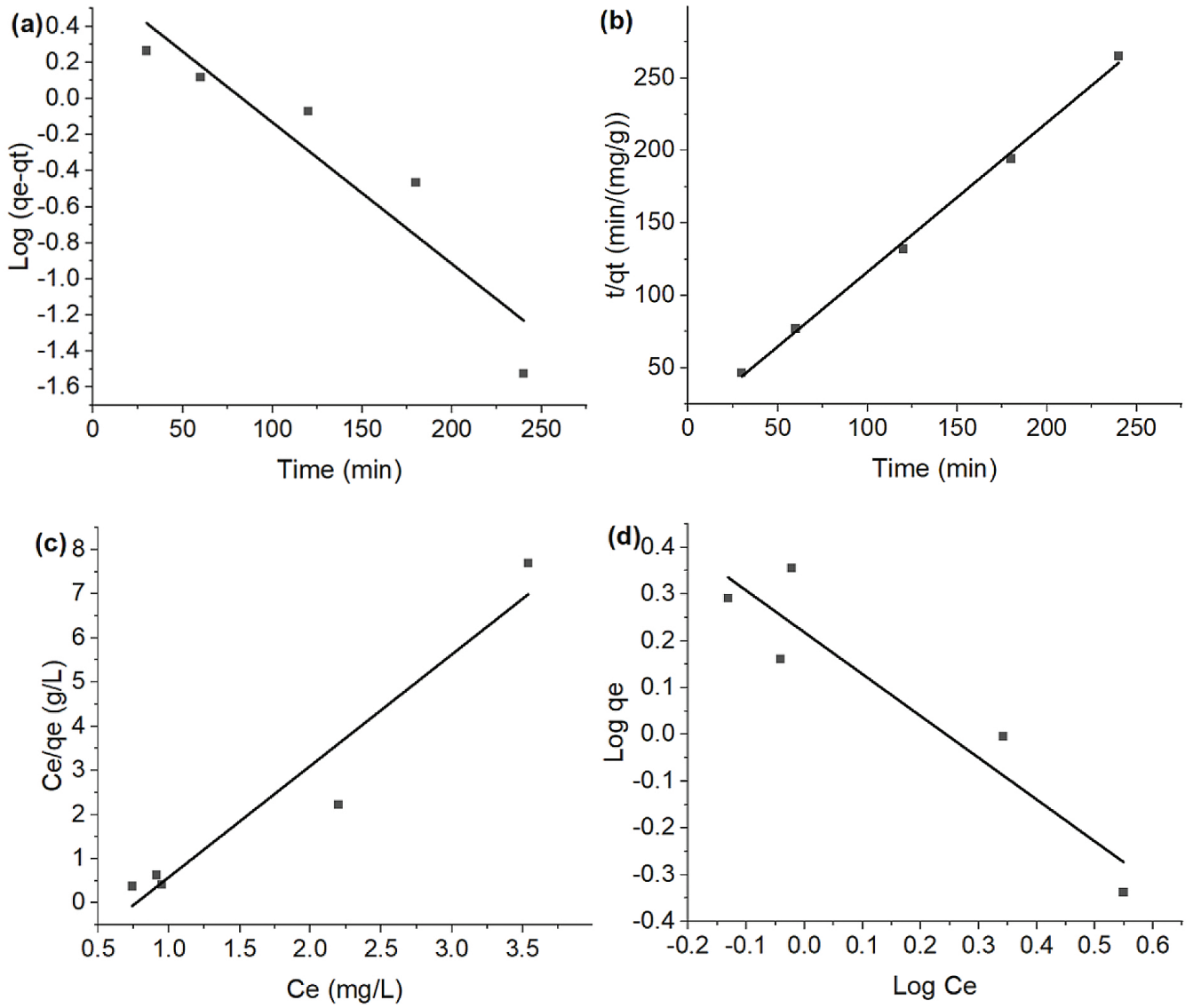

Figure 9. Pseudo first order (a), Pseudo second order (b) kinetics models and Langmuir (c), Freundlich (d) isotherm models for adsorption of methylene blue

Table 1. Kinetics and isotherms parameters for adsorption of methylene blue

Kinetics/Isotherm model	Parameter	Value
Pseudo first order	q_e (Experimental)(mg/g)	0.99
	q_e (Calculated)(mg/g)	4.47
	R^2	0.88
	K_1 (min^{-1})	$1.81x10^{-2}$
Pseudo second-order	q_e (Calculated)(mg/g)	0.97
	R^2	0.99
	K_2 (min^{-1})	$8.03x10^{-2}$
Langmuir	R^2	0.93
	q_m (mg/g)	$3.97x10^{-1}$
	K_a (L/mg)	1.30
Freundlich	R^2	0.88
	N	-1.12
	K_f	1.65

proved to be reusable after showing decrease of 8.17% in adsorption capacity after 5 cycles. The adsorption kinetics suggested that the adsorption process is a chemisorption process since it was favoring the pseudo-second-order reaction while the Langmuir isotherm suggested that it is monolayer sorption at a homogenous surface which also presented us with an idea of the maximum adsorption capacity. Therefore, it is concluded that Luffa MCCs can be effectively utilized in effluent treatment specifically for dye removal.

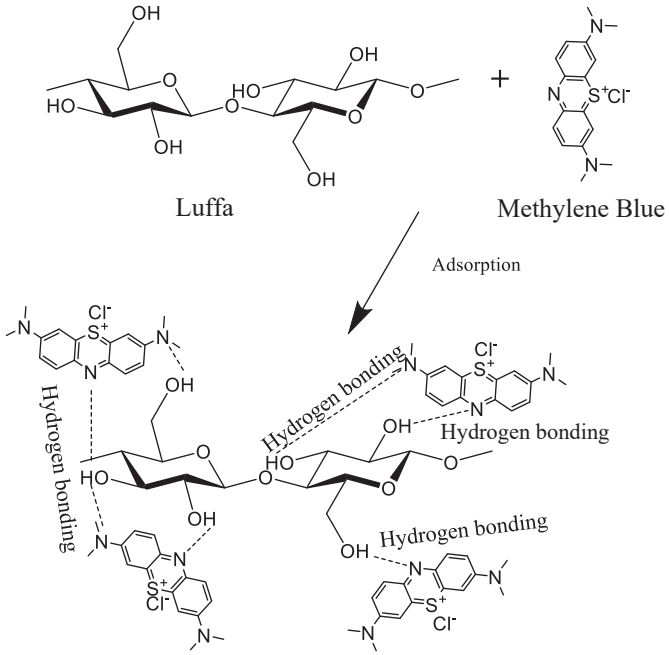

Figure 10. Schematic representation of the adsorption mechanism for methylene blue

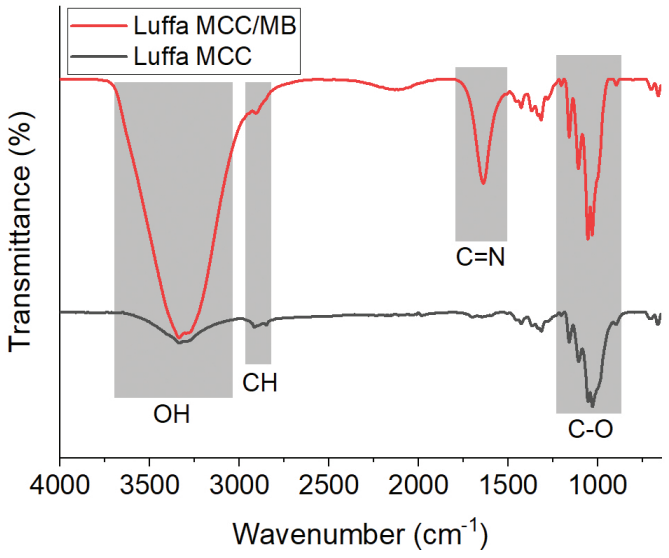

Figure 11 FTIR spectra comparison for Luffa MCC and Luffa MCC/MB

DECLARATION OF COMPETING INTEREST

The authors declare that there is no conflict of interest.

ACKNOWLEDGMENTS

The authors would like to immensely acknowledge National University of Science and Technology, in particular the Department of Fibre and Polymer Materials Engineering for funding this work.

ORCID IDS

Vusumuzi Ngwenya: https://orcid.org/0009-0008-2989-231X
Nqobizitha R. Ndebele: https://orcid.org/0000-0002-3503-7538
Lindani K. Ncube: https://orcid.org/0000-0001-6697-4172
Nkosilathi Z. Nkomo: https://orcid.org/0000-0002-7085-0276
Sithabisiwe Gadlula: https://orcid.org/0009-0005-2700-3361
Lloyd N Ndlovu: https://orcid.org/0000-0002-8856-7970

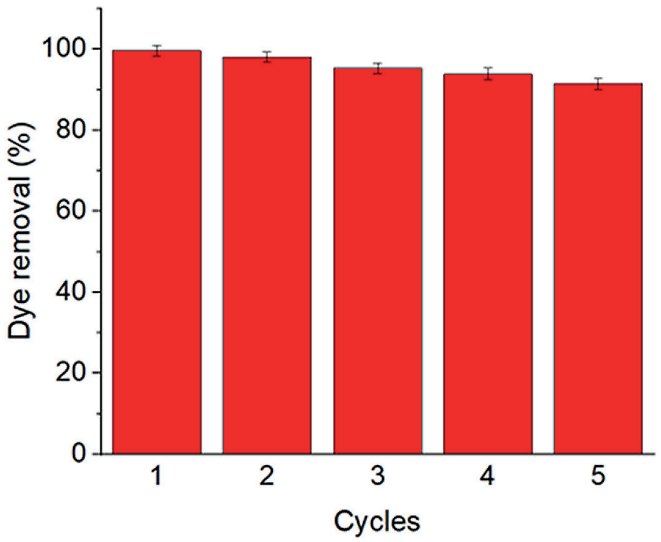

Figure 12 Regeneration studies for methylene blue

REFERENCES

1. Selvaraj V, Karthika TS, Mansiya C, Alagar M. An over review on recently developed techniques, mechanisms and intermediate involved in the advanced azo dye degradation for industrial applications. J Mol Struct. 2021;1224:129195. https://doi.org/10.1016/j.molstruc.2020.129195.
2. Yusuf M. 2019. Synthetic dyes: A threat to the environment and water ecosystem. Textiles and clothing. 1st Edition. Wiley-Scrivener. pp 11–26.
3. Crini G, Lichtfouse E, Wilson LD, Morin-Crini N. Conventional and non-conventional adsorbents for wastewater treatment. Environ Chem Lett. 2019;17(1):195–213. https://doi.org/10.1007/s10311-018-0786-8.
4. Mokhtar N, Aziz EA, Aris A, Ishak W, Mohd Ali NS. Biosorption of azo-dye using marine macro-alga of euchema spinosum. J Environ Chem Eng. 2017;5(6):5721–5731. https://doi.org/10.1016/j.jece.2017.10.043.
5. Natarajan S, Bajaj HC, Tayade RJ. Recent advances based on the synergetic effect of adsorption for removal of dyes from waste water using photocatalytic process. J Environ Sci (China). 2018;65:201–222. https://doi.org/10.1016/j.jes.2017.03.011.
6. Hasanpour M, Hatami M. Photocatalytic performance of aerogels for organic dyes removal from wastewaters: review study. J Mol Liq. 2020;309:113094. https://doi.org/10.1016/j.molliq.2020.113094.
7. Al-Tohamy R, Ali SS, Li F, Okasha KM, Mahmoud YA-G, Elsamahy T, Jiao H, Fu Y, Sun J. A critical review on the treatment of dye-containing wastewater: ecotoxicological and health concerns of textile dyes and possible remediation approaches for environmental safety. Ecotoxicol Environ Saf. 2022;231:113160. https://doi.org/10.1016/j.ecoenv.2021.113160.
8. Katheresan V, Kansedo J, Lau SY. Efficiency of various recent wastewater dye removal methods: A review. J Environ Chem Eng. 2018;6(4):4676–4697. https://doi.org/10.1016/j.jece.2018.06.060.
9. Ahmad A, Mohd-Setapar SH, Chuong CS, Khatoon A, Wani WA, Kumar R, Rafatullah M. Recent advances in new generation dye removal technologies: novel search for approaches to reprocess wastewater. RSC Adv. 2015;5(39):30801–30818. https://doi.org/10.1039/C4RA16959J.
10. Bal G, Thakur A. Distinct approaches of removal of dyes from wastewater: A review. Mater Today Proc. 2022;50:1575–1579. https://doi.org/10.1016/j.matpr.2021.09.119.
11. Bilińska L, Gmurek M. Novel trends in aops for textile wastewater treatment. Enhanced dye by-products removal by catalytic and synergistic actions. Water Resour Ind. 2021;26:100160. https://doi.org/10.1016/j.wri.2021.100160.
12. Adane T, Adugna AT, Alemayehu E. Textile industry effluent treatment techniques. J Chem. 2021;2021:1-14. https://doi.org/10.1155/2021/5314404.
13. Crini G, Lichtfouse E. Advantages and disadvantages of techniques used for wastewater treatment. Environ Chem Lett. 2019;17(1):145–155. https://doi.org/10.1007/s10311-018-0785-9.

14. Kumar PS, Ramalingam S, Sathishkumar K. Removal of methylene blue dye from aqueous solution by activated carbon prepared from cashew nut shell as a new low-cost adsorbent. Korean J Chem Eng. 2011;28(1):149–155. https://doi.org/10.1007/s11814-010-0342-0.
15. Jamali M, Akbari A. Facile fabrication of magnetic chitosan hydrogel beads and modified by interfacial polymerization method and study of adsorption of cationic/anionic dyes from aqueous solution. J Environ Chem Eng. 2021;9(3):105175. https://doi.org/10.1016/j.jece.2021.105175.
16. Momina M, Shahadat M, Isamil S. Regeneration performance of clay-based adsorbents for the removal of industrial dyes: A review. RSC Adv. 2018;8(43):24571–24587. https://doi.org/10.1039/C8RA04290J.
17. Fouladi M, Kavousi Heidari M, Tavakoli O. Development of porous biodegradable sorbents for oil/water separation: A critical review. J Porous Mater. 2022;30(3):1-17. https://doi.org/10.1007/s10934-022-01385-0.
18. Zubair NA, Moawia RM, Nasef MM, Hubbe M, Zakeri M. A critical review on natural fibers modifications by graft copolymerization for wastewater treatment. J Polym Environ. 2021;30(4):1-29. https://doi.org/10.1007/s10924-021-02269-1.
19. Alhijazi M, Safaei B, Zeeshan Q, Asmael M, Eyvazian A, Qin Z. Recent developments in luffa natural fiber composites. Sustainability (Basel). 2020;12(18):7683. https://doi.org/10.3390/su12187683.
20. Ashok K, Kalaichelvan K, Elango V, Damodaran A, Gopinath B, Raju M. Mechanical and morphological properties of luffa/carbon fiber reinforced hybrid composites. Mater Today Proc. 2020;33:637–641. https://doi.org/10.1016/j.matpr.2020.05.716.
21. Chandrashekaraiah P, Kodgire S, Bisht A, Sanyal D, Dasgupta S. Phycoremediation: A promising solution for heavy metal contaminants in industrial effluents. Phycology-based approaches for wastewater treatment and resource recovery. CRC Press; 2021. p. 95–126.
22. Ighalo JO, Adeniyi AG, Eletta OA, Ojetimi NI, Ajala OJ. Evaluation of luffa cylindrica fibres in a biomass packed bed for the treatment of fish pond effluent before environmental release. Sustain Water Resour Manag. 2020;6(6):120–130. https://doi.org/10.1007/s40899-020-00485-6.
23. Heidari MK, Fouladi M, Sooreh HA, Tavakoli O. Superhydrophobic and super-oleophilic natural sponge sorbent for crude oil/water separation. J Water Process Eng. 2022;48:102783. https://doi.org/10.1016/j.jwpe.2022.102783.
24. Jantachum P, Phinyocheep P. A simple method for extraction of cellulose nanocrystals from green luffa cylindrica biomaterial and their characteristics. Polym Int. 2022;72(2):243–251. https://doi.org/10.1002/pi.6463.
25. Macuja JCO, Ruedas LN, España RCN. Utilization of cellulose from luffa cylindrica fiber as binder in acetaminophen tablets. Adv Environ Chem. 2015;2015:243785. https://doi.org/10.1155/2015/243785.
26. Ejikeme PM. Investigation of the physicochemical properties of microcrystalline cellulose from agricultural wastes i: orange mesocarp. Cellulose. 2008;15(1):141–147. https://doi.org/10.1007/s10570-007-9147-7.
27. Saikia D. Studies of water absorption behavior of plant fibers at different temperatures. Int J Thermophys. 2010;31(4-5):1020–1026. https://doi.org/10.1007/s10765-010-0774-0.
28. Kesraoui A, Bouzaabia S, Seffen M. The combination of luffa cylindrical fibers and metal oxides offers a highly performing hybrid fiber material in water decontamination. Environ Sci Pollut Res Int. 2019;26(12):11524–11534. https://doi.org/10.1007/s11356-018-1507-3.
29. Wang H, Liu C, Huang X, Jia C, Cao Y, Hu L, Lu R, Zhang S, Gao H, Zhou W, et al. Ionic liquid-modified luffa sponge fibers for dispersive solid-phase extraction of benzoylurea insecticides from water and tea beverage samples. New J Chem. 2018;42(11):8791–8799. https://doi.org/10.1039/C7NJ04356B.
30. Tanobe V, Flores-Sahagun T, Amico S, Muniz G, Satyanarayana K. Sponge gourd (luffa cylindrica) reinforced polyester composites: preparation and properties. Def Sci J. 2014;64(3):273–280. https://doi.org/10.14429/dsj.64.7327.
31. Chen Y, Su N, Zhang K, Zhu S, Zhao L, Fang F, Ren L, Guo Y. In-depth analysis of the structure and properties of two varieties of natural luffa sponge fibers. Materials (Basel). 2017;10(5):479. https://doi.org/10.3390/ma10050479.
32. Ting Z, Zhiyuan P. Bio-adsorbent from carboxymethyl cellulose and tannin for dye adsorption. J Macromol Sci Part B Phys. 2018;57(3):177–186. https://doi.org/10.1080/00222348.2018.1435491.
33. Melo BC, Paulino FAA, Cardoso VA, Pereira AGB, Fajardo AR, Rodrigues FHA. Cellulose nanowhiskers improve the methylene blue adsorption capacity of chitosan-g-poly(acrylic acid) hydrogel. Carbohydr Polym. 2018;181:358–367. https://doi.org/10.1016/j.carbpol.2017.10.079.
34. Gupta V, Agarwal A, Singh MK, Singh NB. Kail sawdust charcoal: A low-cost adsorbent for removal of textile dyes from aqueous solution. SN Appl Sci. 2019;1(10):1271. https://doi.org/10.1007/s42452-019-1252-3.